

Calculation of the dielectric function for a semi-infinite crystal

S. Brodersen and W. Schattke

Institut für Theoretische Physik und Astrophysik, Christian-Albrechts-Universität zu Kiel, Leibnizstraße 15, D-24098 Kiel, Germany

(Received 7 May 2002; published 3 October 2002)

Calculation of the surface dielectric function (DF) is an important issue for a proper description of many experiments. In this work we present a method for evaluating the DF in half-space geometry avoiding slab or supercell approximations. The method is based on Green's functions and requires no explicit knowledge of wave functions and energies. We test our method by calculating the DF of GaAs(110) and show results for the reflection anisotropy spectroscopy signal.

DOI: 10.1103/PhysRevB.66.153303

PACS number(s): 78.68.+m, 73.20.At

In most experiments aiming at the electronic structure of a surface system, a photon field is involved. In addition, the newer pure optical methods such as reflection anisotropy spectroscopy (RAS) or reflection difference spectroscopy (RDS), there are the classical photoemission (PE) and inverse photoemission (IPE) experiments to name. A theoretical description of these requires the consideration of surface effects on the photon field, which means calculation of the surface dielectric function DF. So far, the surface DF was determined in the supercell approximation.¹⁻³ In particular for PE a proper description of the underlying bulk band structure is mandatory, however. In the following we present a method for evaluating the surface DF for a semi-infinite crystal, which is the most realistic model for a surface.

We calculate the electronic structure within density-functional theory (DFT) in its local-density approximation (LDA). The exchange-correlation potential is due to Ceperley and Alder⁴ as parametrized by Perdew and Zunger.⁵ Wave functions are expanded into linear combinations of atomiclike orbitals (LCAO). For open structures, such as zinc blende, the quality of the basis can be greatly enhanced by additional functions located between the atoms. These off-site functions are necessary to give a good description of the wave function in the interstitial and in the vacuum region. Because of the LCAO ansatz, all-electron calculations pose no problems.

The integrals for the Hamilton and overlap matrix are done by direct integration in real space over the unit cell. This approach has several advantages. First, no expansion of the potential and charge density into auxiliary functions is necessary. Second, it allows for a very flexible basis set, say, extension by plane waves, free Slater or Gaussian orbitals is easily possible. Finally, implementation is very easy and the convergence is controlled by a single parameter, namely, the number of integration points. The unit cell is divided into spheres surrounding the atoms and the remaining interstitial region. Transformation to spherical coordinates within the spheres allows treatment of the singular potential and highly fluctuating core wave functions. For both regions integration is done with a number-theoretical method that traces back to Ellis and Painter⁶ and Zunger and Freeman.⁷ The actual integration points are so-called good lattice points,⁸ which are superior to the earlier methods.

The electronic structure of the half-space is determined by calculating the Green's function $G(\mathbf{r}, \mathbf{r}', \omega)$ with a renormal-

ization algorithm.^{9,10} This algorithm is based on the layer-doubling method for inverting a semi-infinite band-diagonal matrix. Thus only localized basis functions are allowed for expanding the half-space wave functions. From G the density of states (DOS) and with it the Fermi energy are accessible. The surface band structure shows up in the peak dispersion of the k_{\parallel} -resolved DOS. The charge density is calculated from G via a contour integration technique.¹¹ We solve the Poisson equation in a special supercell-like geometry according to Ref. 12. In contrast to the wave functions the potential reaches the bulk values very close beneath the surface. Thus, the supercell approximation is much better justified for calculating the Hartree potential than that for the wave functions. In this way an efficient and accurate self-consistent procedure has been established, leading to the potential, charge density, and band structure of the semi-infinite crystal.

For calculating the dielectric function (DF) a new method had to be developed that accounts for the broken periodicity of the surface system. The usual Adler-Wiser formula,^{13,14} which is the basis for almost all atomistic calculations of optical properties, has to be modified in two ways: First, we cannot expand the DF ϵ in a plane-wave basis because that would impose a three-dimensional periodicity. Instead, we expand the DF into the same basis of localized functions as we do for the wave functions. This approach was tested and validated for bulk crystals.¹⁵ Second, ϵ must be calculated from the Green's function $G(\mathbf{r}, \mathbf{r}', \omega)$ instead of wave functions $\psi_{n\mathbf{k}_{\parallel}}(\mathbf{r})$. This can be achieved by a contour integration in the complex energy plane. With the help of the identity¹⁶

$$\frac{f_{n\mathbf{k}_{\parallel}}}{E_{n\mathbf{k}_{\parallel}} - E_{n'\mathbf{k}'_{\parallel}} - \omega - 2i\eta} = \frac{1}{2\pi i} \oint_C \frac{d\omega'}{(\omega' - E_{n\mathbf{k}_{\parallel}})(\omega' - E_{n'\mathbf{k}'_{\parallel}} - \omega - 2i\eta)}, \quad (1)$$

we are able to reformulate the Adler-Wiser formula in terms of the Green's function

$$G(\mathbf{r}, \mathbf{r}', \omega) = \sum_{n\mathbf{k}_{\parallel}} \frac{\psi_{n\mathbf{k}_{\parallel}}(\mathbf{r}) \psi_{n\mathbf{k}_{\parallel}}^*(\mathbf{r}')}{\omega - E_{n\mathbf{k}_{\parallel}} + i\eta \operatorname{sgn}(E_{n\mathbf{k}_{\parallel}} - E_F)}. \quad (2)$$

Here, $f_{nk_{\parallel}} \in \{0,1\}$ denotes the zero-temperature Fermi occupation number, η a small positive constant, and E_F the Fermi energy. The contour C encloses all poles at energies $E_{nk_{\parallel}}$ below E_F . Poles at $E_{n'k'_{\parallel}} + \omega + 2i\eta$ are outside the integration contour. The remaining real-space integral is given by the vector-valued matrix elements in LCAO representation:

$$A_{ij}^{sq_{\parallel}}(\mathbf{k}_{\parallel}', \mathbf{k}_{\parallel}) = \int d^3r \varphi_{ik_{\parallel}}^*(\mathbf{r}) \varphi_{jk_{\parallel}}(\mathbf{r}) \Phi_{sq_{\parallel}}^*(\mathbf{r}). \quad (3)$$

LCAO basis functions are given by $\varphi_{ik_{\parallel}}(\mathbf{r})$ with i (as well as j and s) a multi-index denoting position and kind of the atom and orbital quantum numbers. The so-called orbital field

$$\Phi_{sq_{\parallel}}(\mathbf{r}) = -\nabla \int d^3r' \frac{\varphi_{sq_{\parallel}}(\mathbf{r}')}{|\mathbf{r}' - \mathbf{r}|} \quad (4)$$

can be calculated by an Ewald technique similar to the method described in Ref. 15. The integral for $A_{ij}^{sq_{\parallel}}$ over the unit rod is done numerically. Because of the localization of the layer Bloch sums $\varphi_{ik_{\parallel}}(\mathbf{r})$ and the orbital field $\Phi_{sq_{\parallel}}(\mathbf{r})$ in the z direction the integration volume can be restricted to a finite range.

Eventually, we arrive at an expression for the DF (in LCAO representation), which is suitable for a practical implementation:

$$\begin{aligned} \overleftrightarrow{\epsilon}_{st}(\mathbf{q}_{\parallel}, \omega) = & S_{st}(\mathbf{q}_{\parallel}) \overleftrightarrow{1} + \frac{i}{4\pi^2} \sum_{\mathbf{k}_{\parallel}}^{\text{1st SBZ}} \text{Tr} \left[\oint_C d\omega' \underline{\underline{A}}^{sq_{\parallel}}(\mathbf{k}_{\parallel} - \mathbf{q}_{\parallel}, \mathbf{k}_{\parallel}) \underline{\underline{G}}(\mathbf{k}_{\parallel}, \omega') \otimes [\underline{\underline{A}}^{tq_{\parallel}}(\mathbf{k}_{\parallel} - \mathbf{q}_{\parallel}, \mathbf{k}_{\parallel})]^+ \underline{\underline{G}}(\mathbf{k}_{\parallel} - \mathbf{q}_{\parallel}, \omega' - \omega - 2i\eta) \right. \\ & \left. - \oint_{C'} d\omega' \underline{\underline{A}}^{sq_{\parallel}}(\mathbf{k}_{\parallel} - \mathbf{q}_{\parallel}, \mathbf{k}_{\parallel}) \underline{\underline{G}}(\mathbf{k}_{\parallel}, \omega' + \omega + 2i\eta) \otimes [\underline{\underline{A}}^{tq_{\parallel}}(\mathbf{k}_{\parallel} - \mathbf{q}_{\parallel}, \mathbf{k}_{\parallel})]^+ \underline{\underline{G}}(\mathbf{k}_{\parallel} - \mathbf{q}_{\parallel}, \omega') \right]. \end{aligned} \quad (5)$$

Here, $\overleftrightarrow{1}$ denotes the unit tensor, \otimes the dyadic product of two vectors, and 1st SBZ the first surface Brillouin zone. The contour C' is the complex conjugate of C . The overlap matrix is given by $S(\mathbf{q}_{\parallel})$ depending on the external two-dimensional wave vector \mathbf{q}_{\parallel} . Due to the localization of the basis functions the $\underline{\underline{A}}$ matrix is band diagonal in the lower indices (like the Hamilton and overlap matrix). Additionally, $\underline{\underline{A}}$ has only a finite number of nonvanishing entries because of the finite range of the orbital field. Thus, multiplications of all these infinite-dimensional matrices can be performed. The matrix of the DF itself is also band diagonal from physical reasons but with a large bandwidth. Practically, we increase the number of evaluated elements of $\overleftrightarrow{\epsilon}_{st}$ until the final results are converged.

The LCAO representation of the DF is well suited for usage in subsequent calculations but not for comparison with experimental results such as RAS signals. Therefore, it is necessary to change to Fourier space. Because of the two-dimensionality this means switching to the Laue representation. The transformation from the LCAO-DF $\overleftrightarrow{\epsilon}_{st}(\mathbf{q}_{\parallel}, \omega)$ to the Laue-DF $\overleftrightarrow{\epsilon}_{G_{\parallel}G'_{\parallel}}(\mathbf{q}_{\parallel}, z, z', \omega)$ can be achieved by matrix multiplications

$$\begin{aligned} \overleftrightarrow{\epsilon}_{G_{\parallel}G'_{\parallel}}(\mathbf{q}_{\parallel}, z, z', \omega) = & \{ \underline{\underline{S}}^{FL}(\mathbf{q}_{\parallel}, z) \underline{\underline{S}}^{-1}(\mathbf{q}_{\parallel}) \underline{\underline{\epsilon}}(\mathbf{q}_{\parallel}, \omega) \underline{\underline{S}}^{-1}(\mathbf{q}_{\parallel}) \\ & \times [\underline{\underline{S}}^{FL}(\mathbf{q}_{\parallel}, z')]^+ \}_{G_{\parallel}, G'_{\parallel}}. \end{aligned} \quad (6)$$

Here,

$$S_{G_{\parallel}s}^{FL}(\mathbf{q}_{\parallel}, z) = \int e^{i(\mathbf{G}_{\parallel} + \mathbf{q}_{\parallel}) \cdot \mathbf{r}'_{\parallel}} \delta(z - z') \varphi_{sq_{\parallel}}(\mathbf{r}') d^3r' \quad (7)$$

denotes the overlap matrix between a Laue basis function and a LCAO function. The inversion of the overlap matrix $S(\mathbf{q}_{\parallel})$ is done with the same renormalization procedure as we use for calculating the Green's function.

Our approach aims at the longitudinal-longitudinal DF. A proper description of the excitations with a transversal electromagnetic field, such as light, is only possible for a vanishing wave vector \mathbf{q}_{\parallel} . For optical experiments, this is indeed fulfilled because the wave vector is much smaller than a typical diameter of the Brillouin zone. Thus, we choose a small value for \mathbf{q}_{\parallel} and interpret the direction of \mathbf{q}_{\parallel} as the polarization direction.

According to Ref. 1 the surface contribution $\Delta R^{\alpha}(\omega)$ to the reflectivity for normal incident light is given by

$$\frac{\Delta R^{\alpha}(\omega)}{R_0(\omega)} = \frac{4\omega}{c} \text{Im} \frac{\Delta \epsilon^{\alpha\alpha}(\omega)}{\epsilon_{\text{bulk}}(\omega) - 1}. \quad (8)$$

Here, c is the speed of light, $R_0(\omega)$ the classical Fresnel reflectivity, and $\epsilon_{\text{bulk}}(\omega)$ the macroscopic DF of the bulk. If we neglect off-diagonal elements of the dielectric tensor, $\Delta \epsilon^{\alpha\alpha}(\omega)$ is related to the macroscopic DF of the surface $\overleftrightarrow{\epsilon}(z, z', \omega)$ by the definition

$$\Delta \epsilon^{\alpha\alpha}(\omega) = \int dz \int dz' [\epsilon^{\alpha\alpha}(z, z', \omega) - \delta(z - z') \epsilon_0(z, \omega)]. \quad (9)$$

If we assume that the vacuum is in the region $z > 0$ and the crystal below $z = 0$, then

$$\epsilon_0(z, \omega) = \epsilon_{\text{bulk}}(\omega) \theta(-z) + \theta(z) \quad (10)$$

is the DF of the sharp crystal-vacuum interface. We approximate the macroscopic surface DF by the $\mathbf{G}_{\parallel} = \mathbf{G}'_{\parallel} = 0$ element

of the Laue representation of the DF. Thus, we neglect local-field effects (LFE) although one would expect a strong influence of LFE at the surface because of the abrupt change of the density. But as was shown in Ref. 3 LFE do not have a pronounced effect on the RAS signal of Si(110). We assume that this will also be the case for GaAs(110), which we take as a test case.

The RAS-signal is given by the difference of the x and y component of the above defined reflectivity:

$$\frac{\Delta R^x(\omega) - \Delta R^y(\omega)}{R_0(\omega)} = \frac{4\omega}{c} \text{Im} \frac{\Delta \epsilon^{xx}(\omega) - \Delta \epsilon^{yy}(\omega)}{\epsilon_{bulk}(\omega) - 1} \quad (11)$$

$$= \frac{4\omega}{c} \text{Im} \frac{\epsilon^{xx}(\omega) - \epsilon^{yy}(\omega)}{\epsilon_{bulk}(\omega) - 1}. \quad (12)$$

We calculate the tensor elements $\epsilon^{xx}(\omega)$ and $\epsilon^{yy}(\omega)$ from the Laue DF:

$$\epsilon^{\leftrightarrow}(\omega) = \int dz \int dz' \epsilon_{G_{\parallel} G'_{\parallel}}^{\leftrightarrow}(\mathbf{q}_{\parallel}, z, z', \omega) \quad (13)$$

by integrating out the z dependence and taking G_{\parallel} and G'_{\parallel} to be zero. This can be viewed as a Fourier transformation in z and z' for vanishing wave vectors q_{\perp} and q'_{\perp} . According to Eq. (6) the z integration is only affected by the overlap matrix $S_{G_{\parallel}}^{FL}(\mathbf{q}_{\parallel}, z)$, which can then be analytically reduced to a one-dimensional integral. The parallel wave vector \mathbf{q}_{\parallel} is taken to be very small and pointing in the x direction for $\epsilon^{xx}(\omega)$ and in the y direction for $\epsilon^{yy}(\omega)$.

As a prototype system we choose the relaxed (110) surface of GaAs. It shows no reconstruction and the electronic and optical properties have already been investigated. Therefore, it is well suited to test our newly developed formula for the DF. We performed two calculations of the electronic structure. For the first one, we choose a large basis set consisting of the atomic $4s$, $4p$, and $4d$ orbitals of As and Ga and off-site functions of s , p , and d types in the interstitial and the vacuum. This leads to the surface band structure depicted by circles in Fig. 1. It is in good agreement with earlier calculations done within the supercell approximation.¹⁷ The theoretical work function of 5.47 eV is very close to the experimental value of 5.5 eV. The second calculation is done with the minimal basis, which means only the occupied $4s$ and $4p$ orbitals of As and Ga are taken. The resulting band structure is depicted by crosses. All the main features, in particular the surface states, are reproduced by the second calculation. Above, say, 5 eV our calculation with the small basis set cannot be trusted.

In order to keep the computational load on a tractable level we evaluated Eq. (5) for the DF with the smaller basis set. The necessary number of integration points for the \mathbf{k}_{\parallel} and energy integration is determined by the value of η . We found 36 \mathbf{k}_{\parallel} points in the surface Brillouin zone and 1400 energy points in the complex plane to be sufficient for a calculation of the DF with $\eta = 0.05$ eV. The convergence behavior of the energy integration is very erratic. The error is rather large before convergence is achieved and very small thereafter. A smoother convergence might be possible with the method described in Ref. 16 at the cost of a further broadening of the

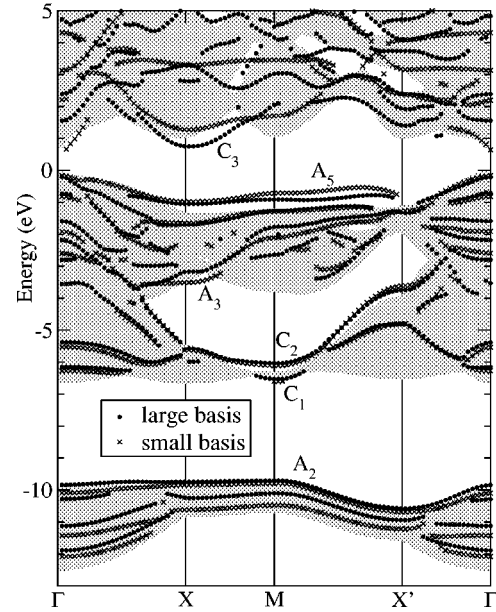


FIG. 1. Surface band structure of GaAs(110). The shaded area denotes the projected bulk band structure that is calculated by a bulk version of the LCAO program.

DF. The matrix dimensions correspond to three unit cells with 12 atoms (one As and one Ga atom per layer and two layers per cell). In order to determine the RAS signal from the DF, the numerical real-space integration of the matrix elements has to be done very precisely. We locate 73 541 integration points in the topmost three unit cells and the vacuum. This is about three times more than is needed for a pure band structure calculation. Still, small inaccuracies in the x and y component of the A matrix lead to an incorrect onset of the RAS signal below the gap energy.

Because of the additional energy integral (which can be done analytically in the bulk case) and the large matrix dimensions, the numerical effort is considerably high. In order to reduce central processing unit (CPU) times, we make an approximation to the dielectric matrix. We found that to a very high degree of accuracy all off-diagonal matrix elements of the LCAO-DF $\vec{\epsilon}$ can be neglected if none of the both indices denote an orbital with s symmetry. This also holds if orbitals of d symmetry are considered. The reason is not yet understood.

From the dielectric matrix the RAS signal is calculated according to Eqs. (6) and (11) by simple matrix multiplications. In Fig. 2 we compare our result with an experimental curve by Esser *et al.*¹⁸ The rather jagged behavior of our result in the higher-energy region is probably due to a too small number of \mathbf{k}_{\parallel} points, which makes it difficult to associate the experimental E'_0 maximum with theory. However, this behavior did not show up in the DF itself. We shifted our curve by 0.34 eV to higher energies to cure the LDA band gap problem. Then, the first three features at 2.7 eV, 2.9 eV, and 3.4 eV are in good correspondence. The following peaks are too low in energy in our spectrum. We identify the experimental minimum at 3.8 eV with the sharp dip at 3.6 eV in our calculation. The shoulder at 4.7 eV (experiment) can be seen in our curve at 4.4 eV. At higher energies we do not

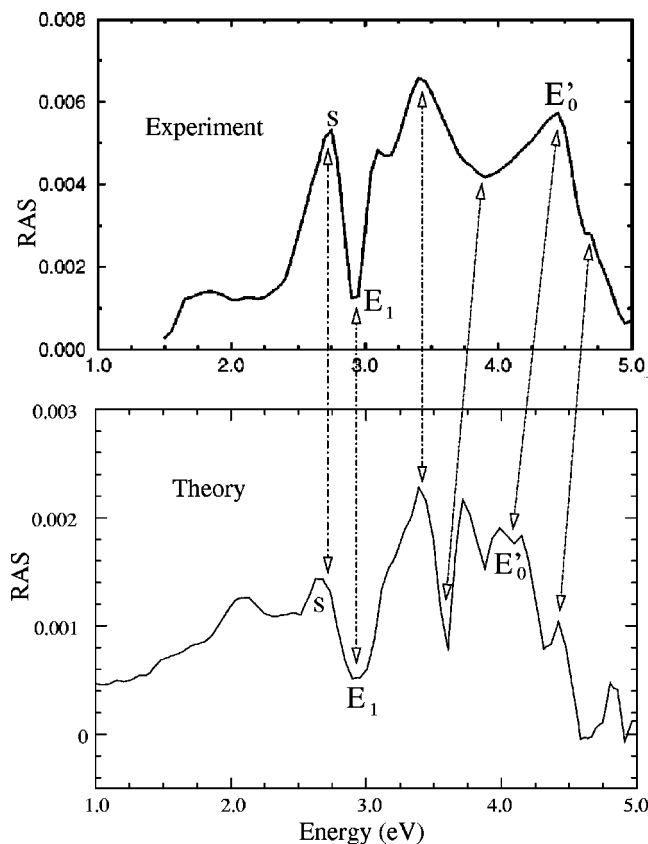


FIG. 2. RAS signal of GaAs(110).

expect good agreement because of the small basis set. The limited basis is also the reason for the small intensity of our RAS signal. Test calculations with a larger basis set (including d orbitals) yield an intensity three times higher. Because of the computational load we were not able to achieve a satisfactory energy resolution with this basis.

In total, we find a rather good agreement between the calculated and measured RAS signal of GaAs(110). The quality is comparable to supercell calculations that are also

within the random-phase approximation (RPA).² For a better description of the relative intensities, excitonic effects have to be taken into account.^{3,19} A better reproduction of the peak positions may be achieved with a larger basis set. The correction of the LDA band energies within a quasiparticle scheme leads to an approximate rigid shift of the RAS signal to higher energies and improves agreement with the measured peak positions.²² In comparison with supercell calculations we do not have convergence problems regarding the thickness of atom and vacuum layers. This problem is addressed in a tight-binding calculation by Del Sole and Onida,²⁰ which shows that around 30 atomic layers are necessary. Whatever method is used, it is difficult to calculate a RAS signal that is converged in all parameters.

In summary, we developed an *ab initio*, self-consistent program for calculating the electronic structure of a semi-infinite crystal. Because of the physically meaningful LCAO basis we are able to perform very accurate or less accurate, very fast calculations. We demonstrate this by the comparison of two band structures of the relaxed GaAs(110) surface. In order to determine the optical properties of a half space, we designed a formula for calculating the DF in the LCAO representation in terms of the Green's function. In this way, the broken periodicity of the half space is fully taken into account. As a test case we calculated the DF and RAS signal of GaAs(110). In spite of the existing theoretical work on the half-space DF,^{21,23} to our knowledge, numerical results have not been reported before. Our approach leads to similar results as supercell calculations. The comparison with experiment shows common characteristic features. It is still hampered due to the numerical effort.

We believe that the half-space geometry is the best model of reality and more work should be concentrated in this direction. In particular, the calculation of optical properties brings the usual slab or supercell approaches to their limits. Our work might be a good starting point for further improvements.

This work was supported by the Deutsche Forschungsgemeinschaft under Contract No. Scha 360/19.

- ¹F. Manghi, R. Del Sole, A. Selloni, and E. Molinari, Phys. Rev. B **41**, 9935 (1990).
- ²O. Pulci, G. Onida, R. Del Sole, and A.J. Shkrebtii, Phys. Rev. B **58**, 1922 (1998).
- ³P.H. Hahn, W.G. Schmidt, and F. Bechstedt, Phys. Rev. Lett. **88**, 016402 (2001).
- ⁴D.M. Ceperley and B.J. Alder, Phys. Rev. Lett. **45**, 566 (1980).
- ⁵J.P. Perdew and A. Zunger, Phys. Rev. B **23**, 5048 (1981).
- ⁶D.E. Ellis and G.S. Painter, Phys. Rev. B **2**, 2882 (1970).
- ⁷A. Zunger and A.J. Freeman, Phys. Rev. B **15**, 4716 (1977).
- ⁸N.M. Korobov, Dokl. Akad. Nauk SSR **132**, 1009 (1960) [Sov. Math. Dokl. **1**, 696 (1960)].
- ⁹M.P. López Sancho, J.M. López Sancho, and J. Rubio, J. Phys. F: Met. Phys. **15**, 851 (1985).
- ¹⁰J. Henk and W. Schattke, Comput. Phys. Commun. **77**, 69 (1993).
- ¹¹R. Zeller, J. Deutz, and P.H. Dederichs, Solid State Commun. **44**, 993 (1982).
- ¹²P. Krüger and J. Pollmann, Phys. Rev. B **38**, 10 578 (1988).
- ¹³S.L. Adler, Phys. Rev. **126**, 413 (1961).
- ¹⁴N. Wiser, Phys. Rev. **129**, 62 (1963).
- ¹⁵S. Brodersen, D. Lukas, and W. Schattke, Phys. Rev. B **66**, 085111 (2002).
- ¹⁶L. Szunyogh and P. Weinberger, J. Phys.: Condens. Matter **11**, 10451 (1999).
- ¹⁷M. Sabisch, P. Krüger, and J. Pollmann, Phys. Rev. B **51**, 13 367 (1994).
- ¹⁸N. Esser, N. Hunger, J. Rumberg, W. Richter, R. Del Sole, and A.I. Shkrebtii, Surf. Sci. **307/309**, A1045 (1994).
- ¹⁹M. Rohlfing and S.G. Louie, Phys. Rev. Lett. **81**, 2312 (1998).
- ²⁰R. Del Sole and G. Onida, Phys. Rev. B **60**, 5523 (1999).
- ²¹R. Del Sole and E. Fiorino, Phys. Rev. B **29**, 4631 (1984).
- ²²O.P. Pulci, G. Onida, R. Del Sole, and L. Reining, Phys. Rev. Lett. **81**, 5374 (1998).
- ²³R. Del Sole, Solid State Commun. **37**, 537 (1981).